

JULITA JAKUBIAK^{*)}, LARS ÅKE LINDÉN^{**)}

Contraction (shrinkage) in polymerization

Part I. FUNDAMENTALS AND MEASUREMENTS

Summary — A review with 58 references covering the areas of shrinkage importance and mechanisms of shrinkage formation, shrinkage types (linear and volumetric) and interrelations, shrinkage measuring methods, *viz.*, static, dynamic, dilatometric, and linometric, laser linear shrinkage measurements, laser scan micrometry, laser interferometry, linear shrinkage measurements of single strands in stereolithography, and dynamic and thermal mechanical analyzer methods.

Key words: polymerization shrinkage, linear and volumetric shrinkage and interrelations, areas of shrinkage importance, shrinkage measuring methods.

Polymerization shrinkage (contraction) is of great importance in:

- Studies on the kinetics of polymerization [1—3].
- Coatings [4, 5]: stresses and consequent defects (buckling, cracking, curling and delamination) caused by shrinkage, limit coating's performance and quality.
- Manufacturing of aspheric lenses, waveguides, gratings and optical fiber coatings; a typical aspheric lens requires a shape accuracy better than 0.1 μm and a surface roughness of less than 0.02 μm [6].
- Stereolithography [7—10].
- Surgical adhesives [13].
- Photocuring of dental restorative resins.

SHRINKAGE FORMATION MECHANISM

There are various causes to shrinkage that occurs during polymerization [12]:

— One major factor is that monomer molecules are located at Van der Waals distances (about 3.4 Å) from one another, whereas in the corresponding polymer the (mono)mer units have moved to within a covalent radius which is approximately 1/3 of the Van der Waals radius (1.34 Å). This causes a shrinkage that is roughly related to the number of (mono)mer units per unit volume that is converted to polymer.

— Change in entropy and in the relative free volumes of the monomer and polymer. Free volume is primarily

determined by the packing efficiency of macromolecules. For example, crystalline (and to some extent semicrystalline) polymers are more closely packed than the corresponding amorphous polymers. Thus, crystalline monomers will shrink less than non-crystalline (liquid) monomers. In the case of methacrylate monomers, it is impossible to avoid shrinkage, which ranges up to 10—16% by volume.

All monofunctional vinyl containing monomers show similar bond changes during polymerization. However, their shrinkage values vary significantly with the molecular weight, elemental composition, and physical state (liquid, solid, crystalline or amorphous) of individual monomers (Table 1) [13, 14].

Table 1. Shrinkage data for various monomers [11]

Monomer	Density at 20°C, g/cc		Shrinkage S_V , %
	monomer	polymer	
Ethylene	0.566 ^{*)}	0.920	66.00
Vinyl chloride	0.919	1.406	34.63
Vinyl bromide	1.512	2.075	27.13
Vinylidene chloride	1.220	1.710	28.65
Vinylidene bromide	2.178	3.053	28.66
Acrylonitrile	0.797	1.170	31.88
Methacrylonitrile	0.800	1.100	27.27
Vinyl acetate	0.932	1.190	21.68
Methyl methacrylate	0.940	1.190	21.01
Ethyl methacrylate	0.911	1.110	17.93
<i>n</i> -Propyl methacrylate	0.902	1.060	14.91
<i>n</i> -Butyl methacrylate	0.889	1.050	15.33
Styrene	0.907	1.059	14.31
Diallyl phthalate	1.175	1.270	7.48
<i>N</i> -Vinylcarbazole	1.110	1.200	7.50
1-Vinylpyrene	1.160	1.230	5.68
Diallyl phthalate prepolymer	1.230	1.270	3.15

^{*)} At -102°C.

^{*)} Department of Chemistry, Jagiellonian University, Ingardena 3, 30-060 Cracow, Poland.

To whom all correspondence should be addressed.

^{**)} Polymer Research Group, Department of Dental Biomaterial Science, Karolinska Institute, Box 4064, S-141 04 Huddinge (Stockholm), Sweden, and Department of Chemistry and Chemical Engineering Technical and Agricultural University, Seminaryjna 3, 85-326 Bydgoszcz, Poland.

Photopolymerization (photocuring) of multifunctional monomers involves complex processes. In the early photocuring period, branched microgel centers are formed, and the crosslinked network of resin components is relatively weak [1—3]. The propagating chains can still flow in the monomer solution and can slide into different positions and assume various orientations in the growing network. At the gel point, the viscous flow of the resin is no longer possible. Therefore, polymer contraction (shrinkage) depends on the flowability of the photocured material. These photocuring process can influence the stress that is being generated. As the photocuring process proceeds, contraction and flow progressively decrease, whereas the resin composite stiffness increases. As a result, the stress begins to grow and can cause adhesion failure.

Linear and volumetric shrinkages

The linear polymerization shrinkage (S_L) can be calculated as

$$S_L = \frac{\Delta l}{l + \Delta l} \cdot 100\% \quad (1)$$

where Δl is the recorded displacement and l the thickness of the sample after polymerization.

The S_L can be converted to volumetric shrinkage (S_V) (with contractions assumed to be isotropical in all x , y and z directions) by the following mathematical expression, in which the relative volumetric contraction is described as the difference between the relative volumes of a cube before and after contraction [15, 16]:

$$S_V = 1^3 - (1 - S_L)^3 = 3S_L - 3S_L^2 + S_L^3 \quad (2)$$

METHODS TO MEASURE THE POLYMERIZATION SHRINKAGE (CONTRACTION)

A number of static and dynamic methods have been developed for measuring the polymerization shrinkage.

Static methods

Static methods are based on measuring the densities by methods such as pycnometry and hydrostatic suspension [17—26]. The volume shrinkage (S_V) can be calculated by the following equation [17, 21, 23—27]:

$$S_V = \frac{V_0 - V_t}{V_0} \cdot 100\% \quad (3)$$

where V_0 and V_t are specific volumes of uncured and cured materials in time (t).

They can be determined as

$$V_0 = \frac{w}{d_0} \quad (4)$$

$$V_t = \frac{w}{d_t} \quad (5)$$

where w is the weight of the cured material, d_0 and d_t are densities of uncured (monomer) and cured (polymer) materials in time (t), respectively.

Liquid densities can be determined with a 1-ml pycnometer to within a precision $\pm 0.1\%$, whereas solid densities can be measured by the water displacement method (hydrostatic weighing technique) on 1- to 2-g samples with a weighing precision of ± 0.1 mg. The volumetric shrinkage (S_V) can be calculated as [27]

$$S_V = \left(\frac{1 - d_0}{d_T} \right) \cdot 100\% \quad (6)$$

The density of water at a desired temperature (d_T) can be found in the literature [28] or evaluated from the following equation [29]:

$$d_T = \frac{999.972}{1 + \sum_{i=1}^{10} 0.01k_i(T - 3.982)^i} \quad (\text{kg} \cdot \text{m}^{-3}) \quad (7)$$

where T is water temperature, °C; and $k_1 = -1.89173965 \cdot 10^{-6}$, $k_2 = 0.080064627$, $k_3 = -0.0866561397$, $k_4 = 0.141326458$, $k_5 = -0.227709811$, $k_6 = 0.305765045$, $k_7 = -0.292859639$, $k_8 = 0.17991657$, $k_9 = -0.0625693644$, $k_{10} = 0.00930376776$ (the use of a programmable calculator is advisable).

Dynamic methods

A number of dynamic methods have been developed to measure shrinkage, *viz.*,

1. Dilatometric measurements of volumetric changes [17, 18, 20—24, 30, 31].
2. Measurements of linear dimensional changes in a thin sample sandwiched between two substrates [15, 16, 30, 32—34].
3. Laser linear shrinkage measurements [9].
4. Laser scan micrometry [35, 36].
5. Laser interferometry [6].
6. Laser measurements of single strands [37].
7. Dynamic (and thermal) mechanical analyzer modified for optical access [38, 39].

In general, the volumetric determinations of curing shrinkage are basically "free shrinkage" measurements and therefore they involve the total (pre- and post-gel) curing contraction, whereas the dimensionless changes in linear curing contraction determinations are more or less "hindered shrinkage" and therefore should be regarded as a post-gel curing phenomenon. For that reason, the various linear shrinkage determinations are often inconsistent.

Dilatometric methods

The volumetric curing shrinkage (S_V) can be measured in the simplest way by using a common NMR tube [11]. In a typical experiment, approximately 1 mL of a reacting sample is placed in the tube. The change of height of the sample in the tube can be recorded with a cathetometer.

A number of devices for determining the volumetric curing shrinkage (S_v) have been reported, most of them based on a mercury dilatometer [17, 30, 40–47] or a water dilatometer [19, 31, 43, 44]. There are two main types of dilatometers: the capillary type [45–50] and the plunger type [47, 51–53]. Dilatometry is laborious and time-consuming and is burdened with data dispersion when used in the low viscosity region. Many other problems exist in using a dilatometer, such as temperature control and viscosity interference. A recording dilatometer for measuring polymerization shrinkage is shown in Fig. 1 [41]. Volume changes are monitored by measuring the height of the mercury column in the vertical portion of the U-tube by means of a linear variable differential transformer (LVDT).

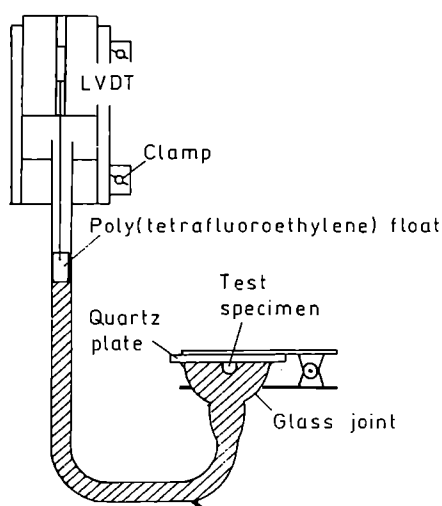


Fig. 1. A schematic diagram of the dilatometer [41]

By assuming the volume shrinkage to vary linearly with monomer conversion, the rate of polymerization (R_p) is expressed in dilatometric studies as [50, 54]

$$R_p = \frac{\Delta V}{V_0} \left[\frac{1}{d_0} - \frac{1}{d_t} \right] M \Delta t \quad (8)$$

where ΔV is the volume change, V_0 is the initial volume, d_0 and d_t are the densities of uncured (monomer) and cured (polymer) material in time (t), respectively, M is the molecular weight of the monomer and Δt is the reaction time.

Linometric methods

Linear polymerization shrinkage can be measured with a "linometer" device that contains a calibrated contactless displacement measuring system, an LVDT transducer (Fig. 2) [15, 32, 38]. The liquid unpolymerized sample is placed between an aluminum disc and a glass cover. Light is switched on and an LVDT transducer measures the vertical displacement of the aluminum disc due to contraction of the sample. The output signal of the measuring system is recorded by a computer. Il-

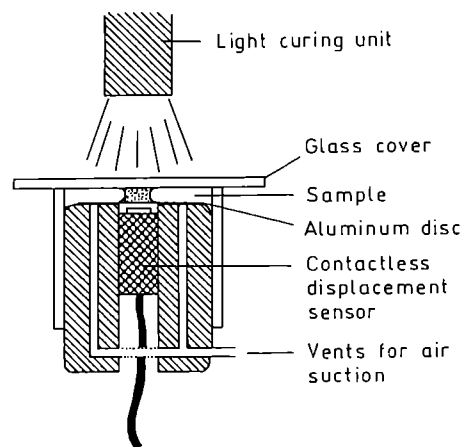


Fig. 2. A schematic diagram of the linometer [15]

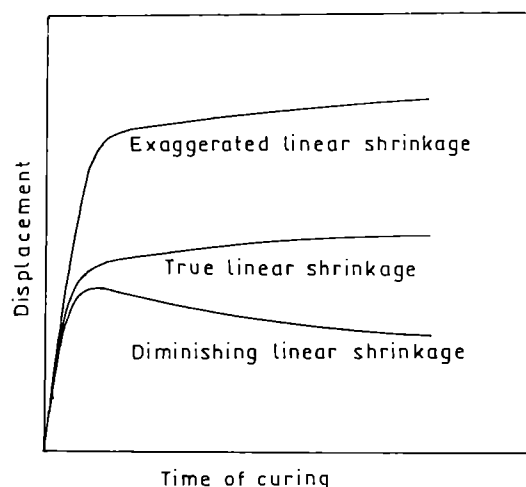


Fig. 3. Kinetic shrinkage curves measured with a linometer [15]

lustrative kinetic shrinkage curves ascertained with the linometer are shown in Fig. 3. A drawback to this method is that, in this sample configuration, stresses will inevitably build up in the polymer layer, notably when the system vitrifies. This will affect the result of a shrinkage measurement.

Laser linear shrinkage measurements

The principle of the experimental equipment is shown in Fig. 4 [9]. The photocurable resin is placed in a vat. An Ar ion laser is used to scan the gap (10 mm) between an immobile and a mobile target. The movement of the mobile target suspended on a fine nylon line is detected with a laser displacement sensor equipped with the data accumulation system.

Laser scan micrometer method

This is a non-contact measuring method of a very high accuracy, $\pm 1 \mu\text{m}$ [35, 36, 55]. A scanning laser beam

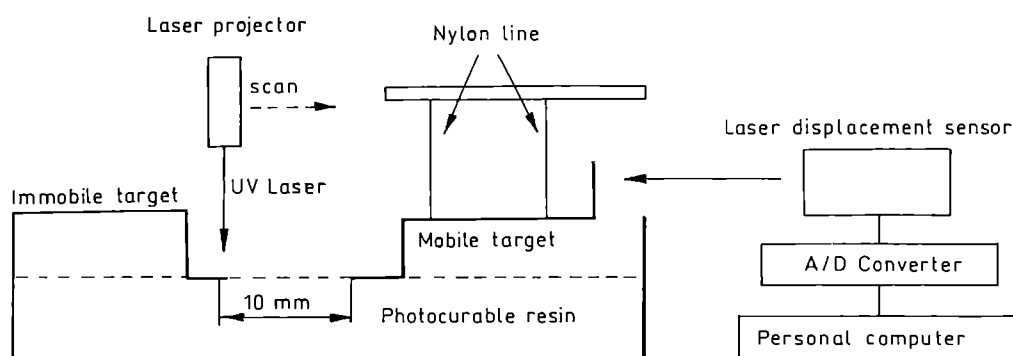


Fig. 4. Laser equipment to measure linear shrinkage [9]

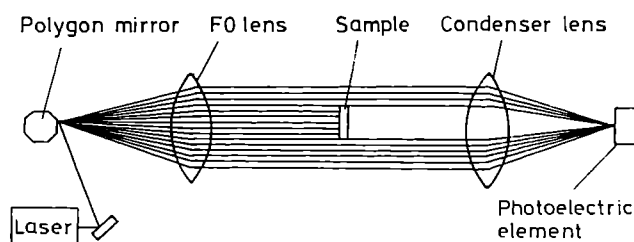


Fig. 5. Diagram of the laser scanning micrometer [35, 36]

is cast over the sample ($\approx 10\text{--}20$ mg, 2–4 mm long, <8 mm in diameter) and its length is determined by measuring the amount of time the specimen obstructs the beam (Fig. 5). The He-Ne laser beam is reflected by a rotating polygon mirror and then collimated by a lens that creates a parallel light flux which scans the specimen. Then, the scanning beam passes through a condenser lens onto a photoelectric element and generates a voltage which corresponds to the intensity of the light. This voltage allows the number of pulses generated to be counted while the beam is being obstructed by the specimen. The number of pulses, which are provided by a clock pulse and totalled by a counter, is proportional to the length of the specimen.

Laser interferometry method

This method is extremely sensitive and can easily detect changes as small as 10 nm [6]. A He-Ne laser beam is used to measure changes in the optical path length of a photocured sample upon irradiation, by using interference of the light reflected at the top and at the bottom of the curable layer (Fig. 6).

The advantage of this method is that it allows to measure the change in the amplitude of the signal due to the increase in the refractive index of the photocured sample. The change in refractive index (n_t) upon polymerization at time (t) is caused by a change in polarizability (α_t) of the sample at time (t). According to the Lorenz-Lorentz equation, the molar refraction (R_{LL}) varies proportionally with α :

$$R_{LL}(t) = \left[\frac{(n_t^2 - 1)}{(n_t^2 + 2)} \right] \left(\frac{M}{d_t} \right) = \frac{4\pi N_A \alpha_t}{3} \quad (9)$$

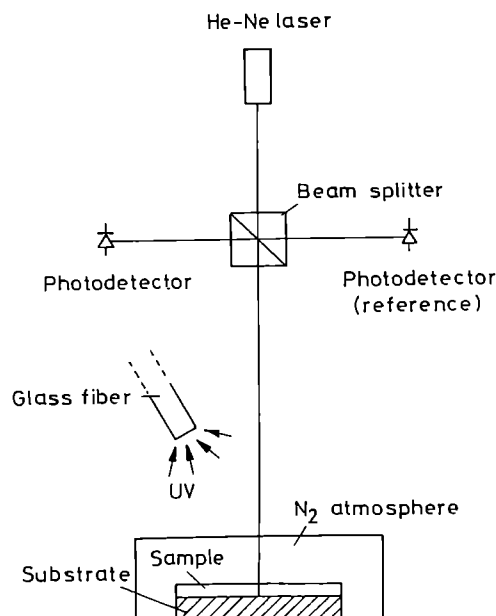


Fig. 6. The laser interferometer for measuring volume shrinkage [6]

where: M is the molecular weight of the monomer, d_t is the density at time (t) and N_A is Avogadro's number.

The change in polarizability (α_t) during polymerization is due to:

- Conversion of double bonds to single bonds, which decreases α_t .
- Shrinkage: the density will increase and thus α_t will increase.

If polarizability (α_t) is assumed to be directly related to the degree of double bond conversion (p_t) (determined in photo-DSC measurements) at time (t), α_t can be represented by the following equation [6]:

$$\alpha_t = \frac{\alpha_m + p_t(\alpha_p - \alpha_m)}{1 - S_{V(t)}} \quad (10)$$

where: α_m and α_p are the polarizabilities of monomer and polymer, respectively, and $S_{V(t)}$ is the volume shrinkage at time (t).

Measurement of the reflected laser light intensity allows to calculate the refractive index, shrinkage and

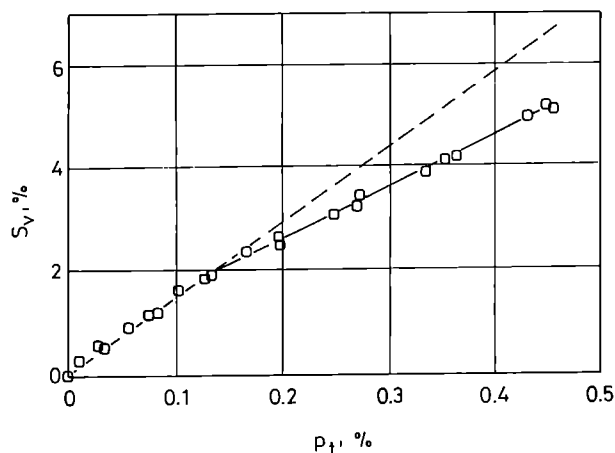


Fig. 7. The relationship between shrinkage (S_V) and double bond conversion (p_t) during photopolymerization of bis(2-hydroxyethyl)bisphenol A dimethacrylate [6]

conversion during photopolymerization. The relationship between shrinkage (S_V) and double bond conversion (p_t) during photopolymerization is shown in Fig. 7.

Linear shrinkage measurements of single strands in 3D photopolymerization (stereolithography)

The principle of the experimental equipment is shown in Fig. 8 [35]. After a laser beam starts from a fixed end, it reaches a free end and the single strand of

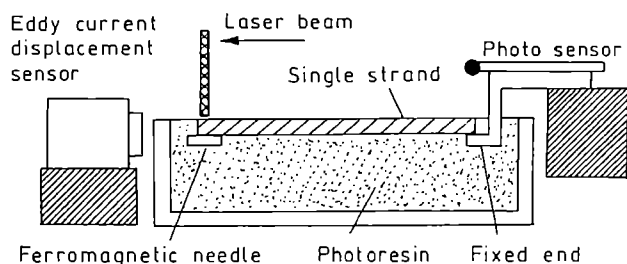


Fig. 8. An experimental setup for single strand measurements [37]

cured resin combines the fixed with the free end, respectively. A non-contact eddy current sensor is used to measure the displacement of a ferromagnetic needle that connects the free end of a single strand. For tracking the beam position and the measuring time, a photo sensor is used to detect the laser traverse during laser scanning. Linear shrinkage (S_L) values is obtained to divide a displacement by the set distance, which is defined as a distance between the fixed and the free end (Fig. 9).

The linear shrinkage ($S_{L(t)}$) of a single strand at time (t) is given as [37]:

$$S_{L(t)} = \int_0^l S_{V(t)}(t + xv) dx \quad (11)$$

where v is the scan speed and x is the path length.

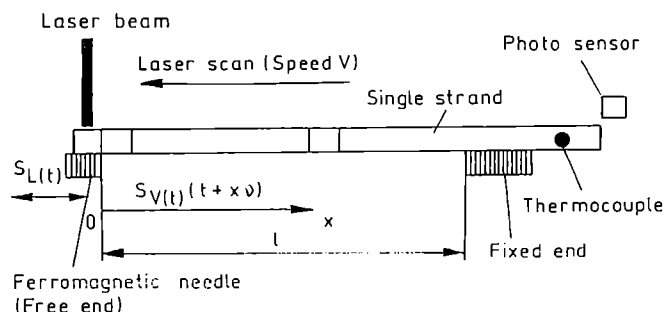


Fig. 9. The definition of measured linear shrinkage ($S_{L(t)}$) at time (t) of a single strand [37]

The volume shrinkage ($S_{V(t)}$) of a single strand at time (t) is given as [37]:

$$S_{V(t)} = -\frac{1}{v} \left(\frac{\partial S_{L(t)}}{\partial t} \right) + S_V(t + l/v) \quad (12)$$

Dynamic (and thermal) mechanical analyzer method

Polymerization shrinkage can be measured by using a dynamic mechanical analyzer (DMA) modified for opti-

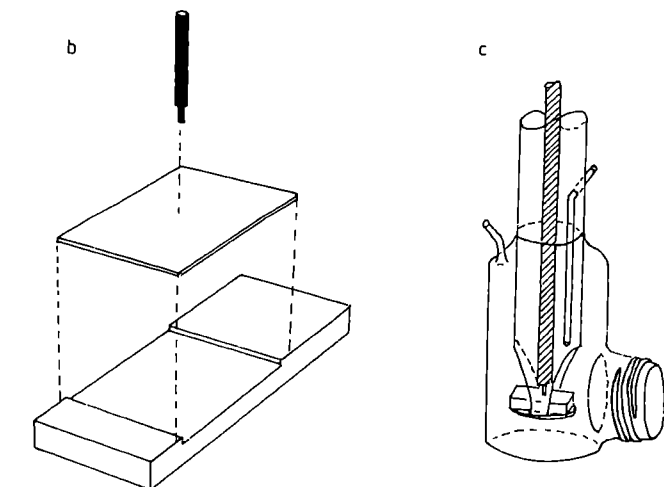
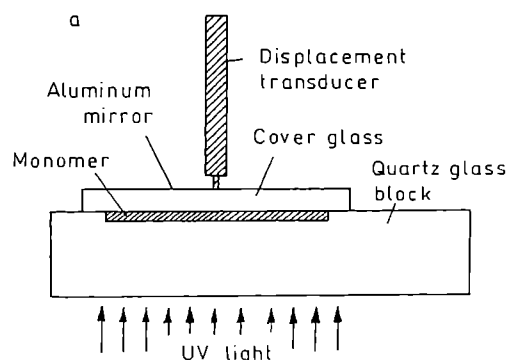


Fig. 10. The thermo-mechanical analyzer (TMA) method for measuring shrinkage: (a) sample sandwich in cross section; (b) disassembled sandwich; and (c) modified TMA instrument [38]

cal access [39]. In the dynamic mode using a probe tip with an oscillating frequency, the entire photoinduced polymerization reaction can be followed with a real time monitor of shrinkage, sample viscosity or modulus [56]. Alternatively, using the thermo-mechanical analyzer (TMA) mode for samples enclosed between glass plates, the probe rests on the top glass plate during the photoreaction and provides an accurate measure of the sample thickness perpendicular to glass plates (Fig. 10) [32, 38, 39]. The overall change in the height is a direct measure of the dimensional change normal to the optical axis (transverse shrinkage). The static method is most useful for evaluating shrinkage in photopolymers since this experiment can utilize the sample in either an unreacted or precured state. This approach can be applied to samples exhibiting a very large (>10%) or a very small (<0.1%) shrinkage [39].

DETERMINATION OF MONOMER CONVERSION DEGREE FROM VOLUMETRIC SHRINKAGE

The degree of double bond conversion (p_i) can be estimated from the volumetric conversion (S_V) by using the following equation [16, 50, 57]

$$p_i = \frac{S_V}{d_0 \Delta V_m c f} \quad (13)$$

where: d_0 is the density of uncured monomer, ΔV_m is the molar volume contraction associated with the polymerization of a mole of double bonds at full conversion ($\Delta V_m = 22.5 \text{ mL/mol}$ for all methacrylates [18, 57, 58]), c is the monomer concentration and f is the number of double bonds in the monomer molecule.

In the case of copolymerization, p_i is given as [57, 58]:

$$p_i = \frac{S_V}{d_i \Delta V_m \sum c_i f_i} \quad (14)$$

where: d_i are the densities of the i -monomer mixtures calculated from the densities of the individual components, $\sum c_i f_i$ is the summation over all concentrations of the i -monomers in the sample (mol/kg) multiplied by the number of double bonds per molecule.

End note: This article has been written by Dr. Julita Jakubiak, Head of an International Joint Project "Mechanisms, kinetics and applications of photopolymerization initiated by visible light photoinitiators", supervised by Prof. J. F. Rabek. Dr. J. Jakubiak spent one year (1998/1999) as post-doc researcher at the Polymer Research Group, Department of Dental Biomaterial Science, Karolinska Institute, The Royal Academy of Medicine, Stockholm, Sweden (directed by Prof. L. Å. Lindén and Prof. J. F. Rabek) and one year (1999/2000) as post-doc researcher at the Laboratoire de Photochimie Generale, CNRS, University of Mulhouse, France (directed by Prof. J. P. Fouassier).

REFERENCES

- [1] Jakubiak J., Rabek J. F.: *Polimery* 2000, **45**, 485. [2] Jakubiak J., Rabek J. F.: *Polimery* 2000, **45**, 659. [3] Jakubiak J., Rabek J. F.: *Polimery* 2001, **46**, 20. [4] Acham N., Crisp J., Holman R., Kakkar S., Kennedy R.: in "Proceedings of the RadTech '95", Maastricht, Netherlands, 1995, p. 71. [5] Payne J. A., Francis L. F., McCormick A. V.: *J. Appl. Polym. Sci.* 1997, **66**, 1267. [6] de Boer, Visser R. J., Melis G. P.: *Polymer* 1992, **33**, 1123. [7] Karrer P., Corbel S., Andre J. C., Loughnot D. J.: *J. Polym. Sci. Polym. Chem.* 1992, **30**, 2715. [8] Jacobs P. F., Ed.: "Rapid Prototyping & Manufacturing", Society of Manufacturing Engineers, Dearborn 1992. [9] Chikaoka S., Ohkawa K.: in "Proceedings of the Asia RadTech '92 Conference", 1993, Tokyo, Japan, p. 468. [10] Jacobs P. F., Ed.: "Sterolithography and other RP&M Technologies: from Rapid Prototyping to Rapid Tooling", Society of Manufacturing Engineers, Dearborn 1996. [11] Berkowicz B. D., Peppas N. A.: *J. Appl. Polym. Sci.* 1995, **56**, 715. [12] Tobolsky A. V., Lonerad F., Roeser G. P.: *J. Polym. Sci.* 1948, **3**, 604. [13] Unterbrink G. L., Muessner R.: *J. Dent.* 1995, **23**, 183. [14] Pezron E., Magny B.: in "Proceedings of the RadTech '96" North America, Nashville, Tennessee, USA, p. 99. [15] de Gee A. J., Feilzer A. J., Davidson C. L.: *Dent. Mater.* 1993, **9**, 11. [16] Venhoven B. A. M., de Gee A. J., Davidson C. L.: *Biomaterials* 1993, **14**, 871. [17] de Gee A. J., Davidson C. L., Smith A.: *J. Dent.* 1981, **9**, 36. [18] Patel M. P., Braden M., Davy K. W. M.: *Biomaterials* 1978, **8**, 53. [19] Hay J. N., Shortall A. C.: *J. Dent.* 1988, **16**, 172. [20] Carvalho R. M., Pereira J. C., Yoshiyama M., Pashley D. H.: *Oper. Dent.* 1966, **21**, 17. [21] Puckett A. D., Smith R. S.: *J. Prosthet. Dent.* 1992, **68**, 56. [22] Lai J. H., Johnson A. E.: *Dent. Mater.* 1993, **9**, 139. [23] Attin T., Buchalla W., Kielbassa A. M., Helwing E.: *Dent. Mater.* 1995, **11**, 359. [24] Rueggeberg F., Tamarhely K. T.: *Dent. Mater.* 1996, **11**, 265. [25] Bogdał D., Boron A., Pielichowski J.: *Polimery* 1996, **41**, 469. [26] Bogdał D., Pielichowski J., Boron A.: *J. Appl. Polym. Sci.* 1997, **66**, 2333. [27] Kurdikar D. L., Pappas N. A.: *Polymer* 1995, **36**, 2249. [28] Riddick J. A., Bunger W. B., Sakano T. A.: "Organic Solvents. Physical Properties and Methods of Purification", Techniques of Chemistry, Volume II, J. Wiley & Sons, New York, Table 0b. [29] Zaitsev I. D., Zozula A. F., Aseev G. G.: Computer Estimation of Physicochemical Property Data of Inorganic Compounds, Moscow, Khimiya 1963. [30] Bausch J. R., de Lange K., Davidson C. L., Peters A., de Gee A. J.: *J. Prosthet. Dent.* 1982, **48**, 59. [31] Bandyopadhyay S.: *J. Biomed. Mater. Res.* 1982, **16**, 135. [32] Kloosterboer J. G., van de Hei G. M. M., Gossink R. G., Dortant G. C. M.: *Polym. Commun.* 1984, **25**, 322. [33] Watts D. C., Cash A. J.: *Dent. Mater.* 1991, **7**, 281. [34] Munksgaard E. C., Hansen E. K., Kato H.: *Scand. Dent. Res.* 1998, **95**, 526. [35] Fano V., Ortalli I., Pizzi S., Noanini M.: *Biomaterials* 1997, **18**, 467. [36] Fano V., Ma W. Y., Ortalli I., Pozela K.: *Biomaterials* 1998, **19**,

1541. [37] Narahara H., Tanaka F., Kishinami T., Igarashi S.: Proc. RadTech '97 Asia Conf., 1997, Osaka, Japan, p. 618. [38] Kloosterboer J. G., Lijten G. F. C. M.: ACS Symp. Ser. 1998, No. 365, p. 409. [39] Bair H. E., Schilling M. L., Colvin V. L., Hale A., Levinos N. J.: *Polym. Preprints* 1998, 78, 230. [40] Smith D. L., Schoonover I. C.: *J. Am. Dent. Assoc.* 1953, 46, 540.
- [41] Penn R. W.: *Dent. Mater.* 1986, 2, 78. [42] Iga M., Takeshige F., Uni T., Torii M., Tsuchitani Y.: *Dent. Mater. J.* 1991, 10, 38. [43] Goldman M.: *Austr. Dent. J.* 1982, 28, 156. [44] Soltesz U., Bath P., Klaiber B.: in "Biological and Biomechanical Performance of Biomaterials" (Eds., Christel P., Meunier A., Lee A. J. C.), Elsevier Science, Amsterdam, 1986, p. 123. [45] Bell C.: *J. Sci. Instr.* 1961, 27, 38. [46] Rubens L., Skochdopole R.: *J. Appl. Polym. Sci.* 1965, 9, 1487. [47] Bartkus E. J., Kroekel C. H.: *Appl. Polym. Symp.* 1970, 15, 113. [48] Nizette J., Desoux V. Z.: *J. Appl. Polym. Sci.* 1971, 15, 1981. [49] Bernatchez P., Goutier D.: *Rev. Sci. Instr.* 1973, 44, 1790. [50] McGinniss V. D., Dusek D. M.: *J. Paint. Technol.* 1973, 46, 23.
- [51] Tung L.: *J. Polym. Sci., Polym. Phys. Ed.* 1967, 5, 319. [52] Hojfors R., Flodin P.: *J. Appl. Polym. Sci.* 1972, 16, 1859. [53] Kinkelaar M., Lee L. J.: *J. Appl. Polym. Sci.* 1992, 50, 37. [54] Anseth K. S., Bowman C. N., Peppas N. A.: *J. Polym. Sci., Polym. Chem.* 1994, 32, 139. [55] Fano V., Ortalli I.: in "Proceedings of the Mediterranean Conference on Medical and Biological Engineering" (Eds., Bracale M., Deroth F.), Vol. I, 1992, Area di Ricerca CNR, p. 113. [56] Bair H. E., Colvin V. L., Schilling M. L.: in "Proceedings of the North American Thermal Analysis Society", 1997, p. 374. [57] Loshaek S., Fox T. G.: *J. Am. Chem. Soc.* 1953, 75, 3544. [58] Eliades G. C., Vougiouklakis G. J., Caputo A. A.: *Dent. Mater.* 1987, 3, 19.

Received 24 IV 2000.